JOURNAL OF CATALYSIS 73, 329–336 (1982)

Band Gap Radiation-Induced Photodesorption from Polycrystalline Powder Surfaces of $SrTiO_3$

NGUYEN VAN HIEU AND DAVID LICHTMAN

Physics Department and Surface Studies Laboratory, University of Wisconsin, Milwaukee, Wisconsin 53201

Received August 22, 1981; revised October 9, 1981

The gas released from an oxygen-saturated powder surface of $SrTiO_3$ upon irradiation in the 310 to 430-nm wavelength region is carbon dioxide. It was found that greater-than-band gap photon energies cause desorption which is linearly proportional to the incident photon intensity, whereas smaller-than-band gap photon energies cause no desorption. The dependence of carbon dioxide photodesorption on net illumination time was also investigated and shows, at first, a rapid decrease in signal followed eventually by a lower constant level of desorption under prolonged exposure to uv radiation. The mechanism proposed is dependent on electron–hole pair production, followed by hole recombination with the bonding electron of a CO_2^- complex leading to thermal desorption of weakly bound CO_2.

I. INTRODUCTION

In 1972, Fujishima and Honda reported that titanium dioxide decomposes water into hydrogen and oxygen when illuminated by photons with energies greater than 3.1 eV (*1*). However, such a photoelectrolytic reaction could only be sustained by the application of an external potential of 0.5 V to the titanium dioxide semiconductor which served as an anode. The reason, as pointed out by Mavroides *et al.* in 1975 (*2*), is that the surface band-bending on the TiO_2 electrode without an applied potential is too small to allow an efficient separation of the photogenerated electron–hole pairs, which is a necessary step in the photoelectrolytic process. In 1976, Mavroides and his coworkers (*3*), and also other investigators (*4, 5*), reported that $SrTiO_3$ and $KTaO_3$ oxides have been found to be able to photoassist the decomposition of water into hydrogen and oxygen in the photoelectrolytic process with no other energy input than that supplied by photons.

The above discovery led to numerous investigations of $SrTiO_3$ in both theoretical and experimental studies. Calculations of the surface energy band of $SrTiO_3$ have been carried out by Wolfram and Morin (*6*), in which they pointed out that the existence of a highly localized *d*-electron surface band density of states in the band-gap region is on the order of $10^{15}/cm^3$. However, this conclusion did not agree with Powell's experimental values of $10^{13}/cm^3$ obtained using the Ultraviolet Photoelectron Spectroscopy (UPS) technique to study reduced and nonreduced $SrTiO_3(001)$ surfaces (*7*). Subsequent calculations by Wolfram and Ellialtioglu in 1977 (*8*), which included Coulomb repulsion among *d* electrons, showed that the position of the *d*-band surface states depends on the position of the Fermi level, which, in turn, depends on the mode of sample treatment. Raising the Fermi level by reduction of the sample, for example, pushes the surface states up into the bulk conduction band so that they remain largely unpopulated.

All modern surface-analysis techniques have been employed to study clean and/or gas-covered $SrTiO_3$ surfaces with different orientations. Low-Energy-Electron Diffraction (LEED) and Auger Electron Spectroscopy (AES) were used to study the surface structure and chemical composition, respectively. Electron energy distributions

0021-9517/82/020329-08$02.00/0

were studied by Energy-Loss-Spectroscopy (ELS) and UPS. Thermal Desorption Spectroscopy (TDS) was used to determine the binding energy between adsorbed gases and substrate, and was also used to study isotopic exchange. The location of hydrogen-bonding sites on $SrTiO_3$ surfaces, which could not be determined by all of the above methods, was revealed by Electron-Stimulated Desorption technique (ESD).

Henrich *et al.* have studied the chemisorption of oxygen on a reduced, Ar-ion bombarded $SrTiO_3(100)$ surface (*9*), and a vacuum-fractured $SrTiO_3(100)$ surface (*10*), under exposures ranging from 0.5 to 10^8 L using UPS, ELS, and AES techniques. They concluded that the band-gap states can be depopulated by exposure to oxygen, and that the band-gap Ti^{3+} *d*-electron states are provided by oxygen vacancies, and not by the $SrTiO_3$ bulk. Lo and Somorjai used LEED, AES, ELS, and UPS to study an Ar-ion bombarded $SrTiO_3(111)$ surface under crystal temperatures ranging from 27 to 600°C (*11*). They found that the concentration of surface Ti^{3+} species decreases with increasing temperature in a reversible manner, and that a significant concentration of Ti^{3+} species is always present on the Sr $TiO_3(111)$ 1×1 surface at room temperature. This Ti^{3+} monolayer makes $SrTiO_3$ superior to TiO_2 in the photoelectrochemical process (does not require applied potential). Chung and Weissbard employed AES, LEED, and UPS techniques (*12*) to study electronic properties of platinum deposited on $SrTiO_3(100)$ surfaces. They pointed out that the Ti^{3+} species is removed by electron loss to the platinum. The charge exchange between $SrTiO_3$ and platinum perhaps plays an important role in the photosynthetic reaction between water and carbon dioxide to form methane as reported by Hemminger *et al.* (*13*). The latter report seems to indicate that no methane formation occurs at the $SrTiO_3$ crystal surface without the inclusion of the platinum foil.

More recently, Ferrer and Somorjai used a combination of UPS, XPS, and TDS techniques to study the adsorption of O_2, H_2, H_2O, O_2, and D_2O on reduced and nonreduced $SrTiO_3(111)$ surfaces under both dark and uv-illuminated conditions (*14, 15*). In general, they found that one monolayer of Ti^{3+} species is present at the surface of reduced $SrTiO_3(111)$, and is depleted under exposure to O_2, H_2, and H_2O gases in the dark. Subsequent band-gap illumination partially restored the initial concentration of Ti^{3+} in the case of O_2 and H_2 exposures, but not in the case of H_2O. Oxygen photodesorption was also detected from the oxygen-covered surfaces. Thermal desorption data indicate the presence of hydroxyl species on the surface that form during water vapor adsorption, and isotropic exchange between the oxygen in the adsorbed $H_2{}^{18}O$ water molecules and the lattice oxygen atom. Bonding of hydrogen species to the $SrTiO_3$ substrate has been studied by Knotek who used ESD technique (*16*). He concluded that hydrogen is adsorbed on the $SrTiO_3$ surfaces as Ti–H, Ti–OH, Sr–H, and to some extent as Sr–OH.

Photocatalytic reactions in the gas phase over $SrTiO_3$ surfaces have been reported in literature; for example, the decomposition of water vapor into hydrogen and oxygen (*17*), the reaction of water vapor and carbon dioxide to form methane (*13*), the production of hydrogen from water vapor-saturated $SrTiO_3$, as well as from platinum vacuum deposited on $SrTiO_3$ crystal surfaces (*18*). The oxidation of CO with O_2 has been studied by Van Damme and Hall (*19*), who found that the oxidation of CO is strongly enhanced by band-gap irradiation.

In this paper, the results of the measurements of photodesorption from oxygen-saturated powder surfaces of $SrTiO_3$ in UHV are reported.

II. EXPERIMENTAL

The ultra-high-vacuum system, detection instrumentation and methods for minimizing the desorption from the stainless-steel

vacuum chamber due to uv irradiation have been described in detail elsewhere (*20, 21*). The base pressure of the system was in the middle 10^{-10} Torr range for this experiment. The strontium titanate powder (purity 98.5%) which was obtained from Ventron Alfa Products Corporation, was mixed with distilled water, spread on an alumina sheet, and then baked in air at 200°C for 4 hr. Samples prepared in this manner were studied by Auger Electron Spectroscopy (AES) and also by Scanning Electron Microscopy. The AES spectrum of $SrTiO_3$ shows the normal strontium, titanium, and oxygen peaks and a carbon surface impurity peak as indicated in Fig. 1. In the Scanning Electron Microscope, the sample powder showed surface structures which indicated a considerable surface to volume ratio. This fact and a relatively large sample surface area (~3.50 cm^2) made these samples especially suitable for sensitive photodesorption studies since photodesorption signals available per unit area are usually small (*22*).

After initial evacuation to the 10^{-8} Torr range (1 Torr = 133.3 Nm^{-2}), residual impurities deposited on the sample surface during preparation were removed by a brief heating at ~200°C. The sample was indirectly heated by passing a current through a tantalum heater foil which held the sample. The sample temperature was monitored by an alumel–chromel thermocouple which was mechanically attached to the front. The sample is pretreated by exposure to research grade oxygen at a pressure of one atmosphere for 15 min while the sample temperature is maintained at ~100°C.

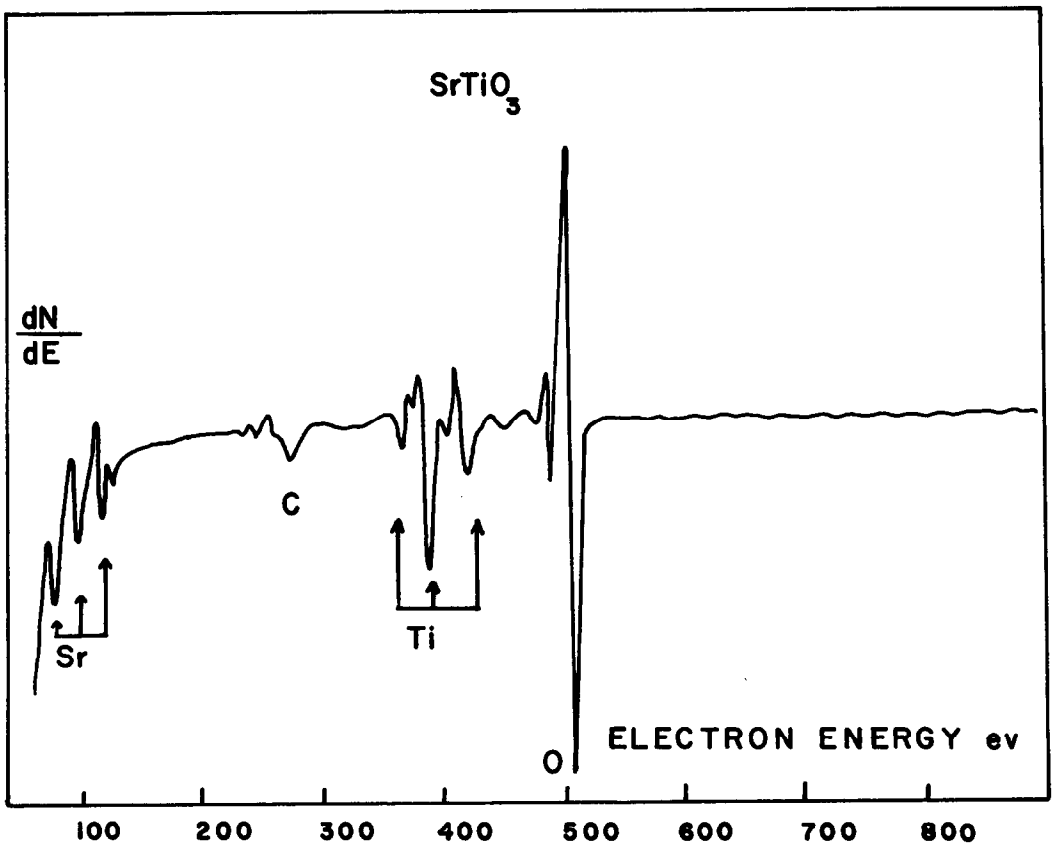

FIG. 1. Auger spectrum of $SrTiO_3$, experimental parameters: E_p = 8 keV, I_p = 10^{-7} A, modulation voltage = 5 V peak-to-peak.

Band-gap radiation (>3.1 eV) was provided by a 1000-W high-pressure xenon–mercury lamp that was placed in an air-cooled housing equipped with a fused quartz condenser lens system to focus the incident light on the 3.5 cm^2 sample area. A 2-in.-thick distilled-water filter was also used to absorb infrared radiation. The incident photon flux, measured by a radiometer (International Light Company) ranged from 4.2×10^{15} to 2×10^{16} photons per cm^2-sec. All data were taken with 1-s illumination pulses using an electronic photographic shutter mechanism.

III. RESULTS

3.1. Analysis of Photodesorbing Signal

The production of gases from an oxygen-saturated powder surface of $SrTiO_3$ during a 1-sec illumination interval is shown in Fig. 2. The 3650-Å line of a xenon–mercury lamp at a flux of 1.6×10^{16} photons per cm^2-sec was used as a uv source. The signal

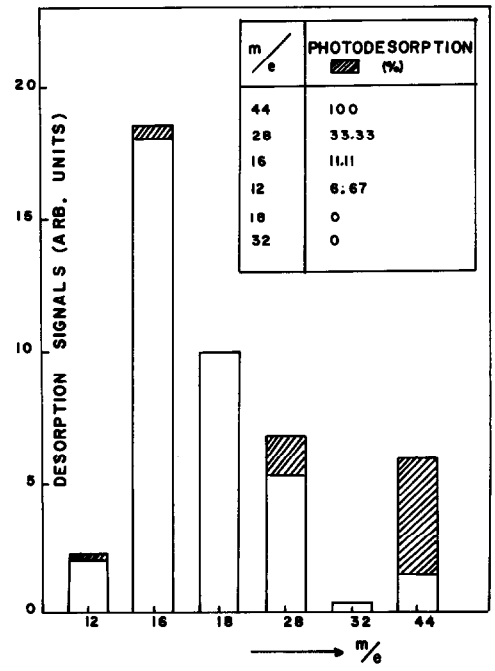

FIG. 2. Relative signal strengths of 12, 16, 18, 28, 32, 44 peaks before and after 1-sec illumination, using 365-nm line at a flux of 1.626×10^{16} photons per cm^2-sec as a uv source.

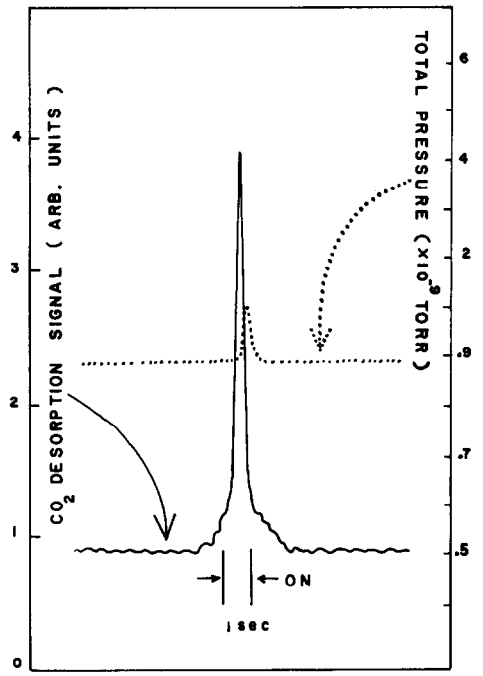

FIG. 3. A typical chart recorder output of the carbon dioxide signal (solid line) together with the total pressure change (dotted line and slightly shifted to the right) during 1-sec illumination using 365-nm line at a flux of 1.626×10^{16} photons per cm^2-sec.

peaks at the mass-to-charge ratios (m/e) of 12, 16, 28, and 44 which corresponds to carbon, atomic oxygen, carbon monoxide, and carbon dioxide, respectively, are observed to increase. No change was observed at m/e values of 18, 32 which are respectively water vapor and molecular oxygen. A detailed mass analysis of carbon dioxide had been reported earlier (*20*), indicating that the change in m/e values of 12, 16, 28 (C, O, CO) are due to the cracking pattern of CO_2 produced in the mass spectrometer's ion cage. Therefore, carbon dioxide is the only detectable photodesorption species. It should be mentioned that one reason for monitoring these m/e values is to compare the present results with previous studies of band-gap-induced photodesorption from TiO_2 powders (*23–25*) titanium oxide surfaces (*20*), and TiO_2(001) surfaces (*26*). A typical chart recorder output is displayed in Fig. 3, showing the rela-

tive change of the carbon dioxide peak (solid line) with the total pressure change (dotted line) during a 1-sec illumination interval.

3.2. Carbon Dioxide Photodesorption Signal as a Function of Photon Wavelength

To determine the carbon dioxide photodesorption signal as a function of photon wavelength, commercial interference filters (Klinger Scientific Corp.) were used to isolate the 3130 Å (3.962 eV), 3340 Å (3.710 eV), 3650 Å (3.397 eV), 4047 Å (3.064 eV), and 4358 Å (2.845 eV) spectral lines from a 1000-W xenon–mercury lamp. The incident photon flux at each wavelength was measured with a radiometer and has values of 4.2×10^{15}, 5.2×10^{15}, 1.6×10^{16}, 1.3×10^{16}, and 1.9×10^{16} photons per cm^2-sec, repectively. The results of these experiments are plotted in Fig. 4 (after normalization of incident photon flux). From Fig. 4, one can see that there is a detectable signal at the 3650-Å wavelength, but no carbon dioxide photodesorption signal was observed at the 4047-Å wavelength.

A similar experiment as above was carried out, but this time high-pass Corning glass filters were used instead, and results are shown in Fig. 5. Figure 5 indicates that the relative carbon dioxide desorption signal decreases with increasing cutoff wavelength of these filters from 3200 to 4000 Å.

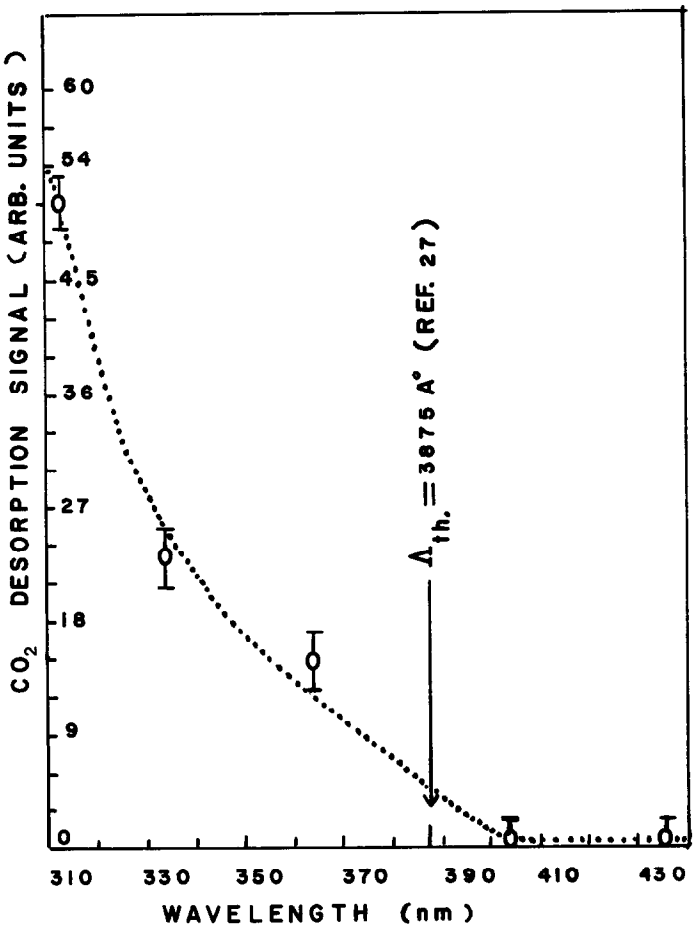

FIG. 4. Carbon dioxide photodesorption as a function of photon wavelength.

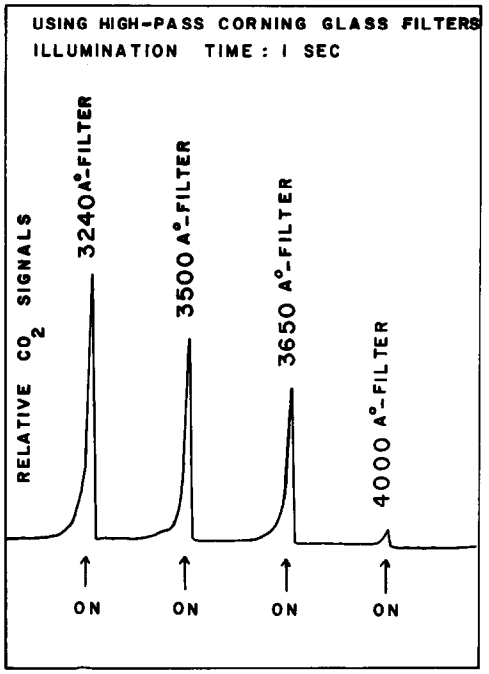

FIG. 5. Relative signal strengths of carbon dioxide versus high-pass Corning glass filters with 1-sec illumination time.

A small carbon dioxide desorption signal was still detected with the 4000-Å high-pass filter (λ_{cutoff} = 4000 Å). Since these high-pass Corning glass filters are not perfect cutoff, therefore some photons at wavelengths less than cutoff = 4000 Å (e.g., energies > 3.1 eV) still transmit through the 4000-Å high-pass filter and cause some desorption. The band-gap energy of 3.17 eV for $SrTiO_3$ has been reported in literature (*27*), and corresponds to the wavelength value of ~3875 Å. The measured threshold as seen in Fig. 4 clearly relates to the band-gap of the $SrTiO_3$.

Two basic observations have been mentioned above, namely: (1) carbon dioxide is the only detectable photodesorption species, (2) no signal was detected at photon energies less than ~3.1 eV, suggesting that the oxidation of carbon impurities by adsorbed oxygen, together with the capture of an electron from the conduction band, forms a CO_2^- complex. An incident photon of energy equal to or greater than that of the band gap is absorbed by this material creating electron–hole pairs. Holes produced near the surface can migrate to the surface and recombine with the chemisorbed CO_2^- complex, breaking the chemisorption bond, resulting in the thermal desorption of the CO_2 molecule. This band-gap-induced photodesorption process was reviewed recently in Ref. (*28*).

3.3. Carbon Dioxide Photodesorption Signal Versus Photon Intensity

To check the dependence of carbon dioxide desorption signal on photon intensity, copper meshes were used as neutral filters to reduce the intensity of the 3650-Å line at an original flux of 1.6×10^{16} photons per cm^2-sec. Incident photon intensities, after passing through copper meshes, were measured by a radiometer, and the results of these runs are plotted in Fig. 6. To within

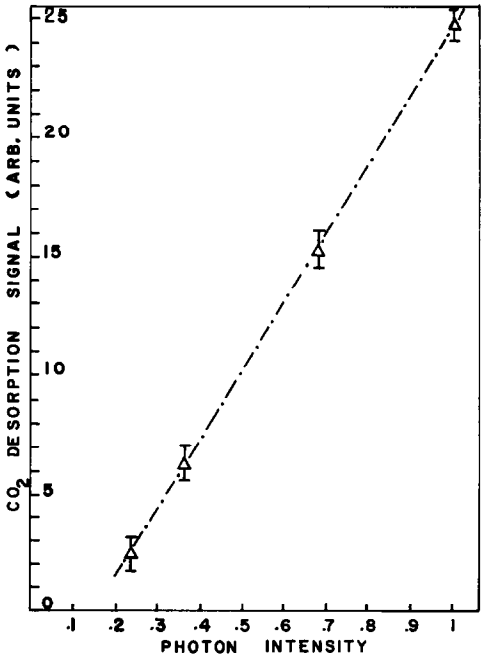

FIG. 6. Carbon dioxide photodesorption signals versus uv photon intensity, using 365-nm line at a flux of 1.626×10^{16} photons per cm^2-sec with 1-sec illumination time.

experimental error (see error bars in Fig. 6), the relationship is linear which indicates that the carbon dioxide signal is a true photon-induced desorption, and not a photon-induced surface heating effect, since the latter should show a highly superlinear dependence [α exp − (activation energy/kT)] (*29*).

3.4. Carbon Dioxide Photodesorption Signal as a Function of Illumination Time

Figure 7 shows the time decay of the carbon dioxide photodesorption signal using the 3650-Å line at a flux of 1.6×10^{16} photons per cm²-sec. First observations indicate that the carbon dioxide photodesorption signal decreases rapidly in the first 150 sec, and afterward becomes constant with time (Fig. 7). Similar observations from several semiconductors such as ZnO (*30*), TiO_2 (*25*), and V_2O_5 (*21*) have been reported earlier from this laboratory. In the ultra-high-vacuum environment readsorption of oxygen is not available to reduce the accumulation of negative charge which forms by photogenerated electrons. This charge layer in turn reduces the probability of recombination of the CO_2^- ion complex with photogenerated holes. Consequently, the signal decreases with illumination time finally reaching an equilibrium value (*35*).

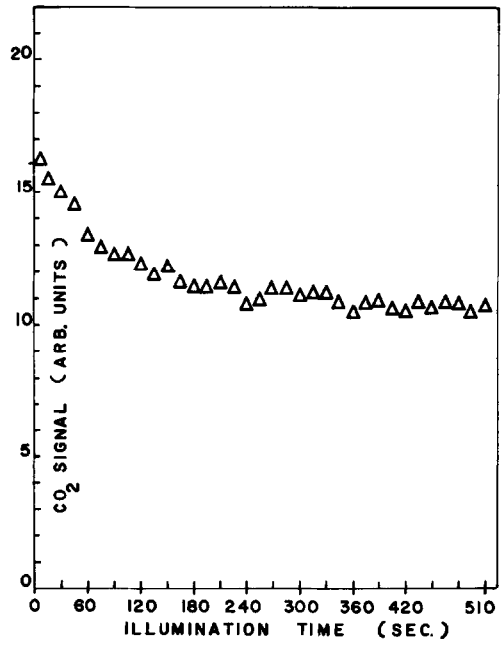

FIG. 7. Relative carbon dioxide photodesorption signals versus net illumination time, using 365-nm line at a flux of 1.626×10^{16} photons per cm²-sec with 1-sec illumination interval.

IV. SUMMARY

In this laboratory, extensive studies have been done on photodesorption from three basic different types of materials: Polycrystalline powder samples of ZnO (*31*), TiO_2 (*25*), V_2O_5 (*21*), single crystal samples of ZnO (*30*), TiO_2(001) rutile structure (*26*), and oxide surfaces of chronium (stainless steel) (*32*), niobium (*33*), titanium (*20*), and vanadium (*21*), and now powder samples of $SrTiO_3$. The following conclusions resulted from these studies: (1) adsorption of oxygen (~15 min at atmospheric pressure oxygen) is a necessary step for photodesorption experiments, (2) carbon dioxide is the desorbing species from these surfaces, (3) photon energy equal to or greater than the band-gap energy is required to cause desorption, (4) the carbon dioxide photodesorption signal depends linearly on incident photon flux, and (5) finally there are direct correlations among illumination time, surface carbon content, and photodesorption activities from these materials (*21, 34*). The behavior of $SrTiO_3$ seems essentially identical to that of the other sample metal oxides.

Experiments are now in progress to study photodesorption, and surface conductivity with silicon and germanium systems, and it is hoped that these results, together with previous results, will enable the establishment of a clear, complete band-gap photon-induced desorption mechanism for semiconductor materials.

REFERENCES

1. Fujishima, A., and Honda, K., *Nature (London)* **37**, 238 (1972).
2. Mavroides, J. G., Tcherner, D. I., Kafalas, J. A.,

and Kolesar, D. F., *Mater. Res. Bull.* **10,** 1023 (1975).
3. Mavroides, J. G., Kafalas, J. A., and Kolesar, D. F., *Appl. Phys. Lett.* **28,** 231 (1976).
4. Wrighton, M. S., Ellis, A. B., Wolczanski, P. T., Morse, D. L., Abrahamson, H. B., and Ginley, D. S., *J. Amer. Chem. Soc.* **98,** 2774 (1976).
5. Watanabe, T., Fujishima, A., and Honda, K., *Bull. Chem. Soc. Japan* **49,** 355 (1976).
6. Wolfram, T., and Morin, F. J., *Appl. Phys.* **8,** 125 (1975).
7. Powell, R. A., and Spicer, W. E., *Phys. Rev. B* **13,** 2601 (1976).
8. Wolfram, T., and Ellialtioglu, S., *Appl. Phys.* **13,** 21 (1977).
9. Henrich, E., Dresselhaus, G., and Zeiger, H. J., *J. Vac. Sci. Technol.* **15,** 534 (1978).
10. Henrich, E., Dresselhaus, G., and Zeiger, H. J., *Phys. Rev. B* **17,** 4908 (1978).
11. Wei Jen Lo and Somorjai, G. A., *Phys. Rev. B* **17,** 4942 (1978).
12. Yip-wah Chung and Weissbard, W. B., *Phys. Rev. B* **20,** 3456 (1979).
13. Hemminger, J. C., Carr, R., and Somorjai, G. A., *Chem. Phys. Lett.* **57,** 100 (1978).
14. Ferrer, S., and Somorjai, G. A., *Surf. Sci.* **94,** 41 (1980).
15. Ferrer, S., and Somorjai, G. A., *Surf. Sci.* **97,** L304 (1980).
16. Knotek, M. L., *Surf. Sci.* **101,** 334 (1980).
17. Chung, Y. W., Lo, W. J., Hemminger, J. C., and Somorjai, G. A., Lawrence Berkeley, Laboratory Report Number LBL-6627.
18. Wagner, F. T., Ferrer, S., and Somorjai, G. A., *Surf. Sci.* **101,** 462 (1980).
19. Van Damme, H., and Hall, W. K., *J. Catal.*, in press.
20. Hieu, N. V., and Lichtman, D., *Surf. Sci.* **103,** 535 (1981).
21. Hieu, N. V., and Lichtman, D., *J. Vac. Sci. Technol.* **18,** 49 (1981).
22. Lichtman, D., and Shapira, Y., *CRC Critical Rev. Solid State Mater. Sci.* **8,** 93 (1978).
23. Juillet, F., Formenti, M., Lissatchenka, H., Martin, J. R., Meriandeau, P., and Teichner, S. J., *J. Vac. Sci. Technol.* **9,** 947 (1972).
24. Juillet, F., Thevenet, A., and Teichner, S. J., *Japan J. Appl. Phys. Suppl. Vol 2 pt 2* (1974).
25. Cox, S. M., and Lichtman, D., *Surf. Sci.* **54,** 675 (1976).
26. Korchak, N., Krylov, O. V., Hieu, N. V., Lichtman, D., Fu, Chia-Min and Hall, W. K., submitted for publication.
27. Blazey, K. W., *Phys. Rev. Lett.* **27,** 146 (1971).
28. Lichtman, D., *Surf. Sci.* **90,** 579 (1979).
29. Geneguand, P., *Surf. Sci.* **25,** 643 (1971).
30. Shapira, Y., Cox, S. M., and Lichtman, D., *Surf. Sci.* **54,** 43 (1976).
31. Shapira, Y., Cox, S. M., and Lichtman, D., *Surf. Sci.* **50,** 503 (1975).
32. Fabel, G. W., Cox, S. M., and Lichtman, D., *Surf. Sci.* **40,** 571 (1973).
33. Lichtman, D., and Lin, T., Proc., 7th Intern. Vac. Congr. and 3rd Intern. Conf. Solid Surfaces (Vienna, 1977).
34. Lichtman, D., and Shapira, Y., *J. Nucl. Mater.* **63,** 184 (1976).
35. Shapira, Y., McQuistan, R. B., and Lichtman, D., *Phys. Rev. B* **15,** 2163 (1977).